nature physics

SUPPLEMENTARY INFORMATION

DOI: 10.1038/NPHYS3527

Characterization of collective ground states in single-layer $NbSe_2$

Miguel M. Ugeda*, Aaron J. Bradley, Yi Zhang, Seita Onishi, Yi Chen, Wei Ruan, Claudia Ojeda-Aristizabal, Hyejin Ryu, Mark T. Edmonds, Hsin-Zon Tsai, Alexander Riss, Sung-kwan Mo, Zahid Hussain, Dunghai Lee, Alex Zettl, Zhi-Xun Shen and Michael F. Crommie*.

*Correspondence to: mmugeda@berkeley.edu and crommie@berkeley.edu.

This PDF file includes: **Page**

© 2015 Macmillan Publishers Limited. All rights reserved

1. ARPES characterization of the monolayer and 5ML- $NbSe_2$

The *in-situ* angle-resolved photoemission spectroscopy (ARPES) measurements were performed at the HERS endstation of beamline 10.0.1 at the Advanced Light Source, Lawrence Berkeley National Laboratory. Samples were cooled to ~60K during measurement. The size of the beam spot on the sample was ~150 μm × 200 μm, and the photon energy was 50 eV with energy and angular resolution of 25 meV and 0.1^{o}, respectively. Fig. S1a shows the geometry of the ARPES measurement. The plane of incidence is along the Γ-M (k_y) direction of the substrate BLG, and the detector slit of the analyzer is along the Γ-K(k_x) direction of the substrate BLG. Two types of photon polarizations were used. In one polarization the photon electric field was perpendicular to the plane of incidence (i.e. *s*-polarization). In the other polarization, the photon electric field was 20° out of the plane of incidence (a mixture of *s*-polarization and *p*-polarization referred to as *sp-mixed* polarization).

Fig. S1b shows the hexagonal 2D Brillouin zone (black dotted hexagon) and a schematical drawing of the Fermi surface (orange dotted lines) for single-layer $NbSe_2$, with a near-hexagon pocket at the Γ point and a near- triangle pocket at each of the six K points. Figs. S1c and S1d show Fermi surface maps taken with *s*-polarized photons and *sp*-mixed polarized photons, respectively. We found that the $NbSe_2$ films contain randomly rotated domains with two dominant, preferred orientations. The two dominant orientations, separated by a 30° difference, are depicted in figs. S1c and S1d as dotted orange hexagons, in good overall agreement with the Fermi surface mapping data. The randomly rotated domains were also observed in the scanning tunneling microscopy (STM) measurements (see fig. S2).

Even though the ARPES spectra along Γ-M and Γ-K directions were mixed due to the randomly rotated domains, we still can distinguish the Γ-M and Γ-K bands by using different photon

© 2015 Macmillan Publishers Limited. All rights reserved

polarizations[1]. Fig. S1e and S1g are the ARPES spectra of a monolayer $NbSe_2$ film taken with *s*-polarization and *sp-mixed* polarization, respectively. The corresponding second-derivative spectra are provided for enhanced visibility (figs. S1f and S1h). Using *s*-polarized photons, only the Γ-K band (depicted by the orange dotted line) can be observed in figs. S1e and S1f; using *sp-mixed* polarized photons, both the Γ-K band and the Γ-M band (depicted by dotted and dot-dashed orange lines, respectively) can be observed in figs. S1g and S1h. The photon polarization dependence of the ARPES spectra is a consequence of the orbital character of the bands; the dipole matrix element in ARPES becomes larger when the photon polarization aligns with the direction of preferred electron population of particular orbitals. Therefore, the disappearance of the Γ-M band and the clear signal from the Γ-K band in the *s*-polarization spectra indicate that the Γ-K band is mainly composed of in-plane orbitals such as the $d_{x^2-y^2}$ and d_{xy} orbitals while the Γ-M band, only visible in *sp-mixed* polarization, is mainly composed of out-of-plane d_{z^2} orbitals. These observations are in good agreement with the previously calculated orbital character of the electronic bands of $NbSe_2$[2]. Importantly, we found only one band crossing the Fermi level for single-layer $NbSe_2$, which agrees well with recent calculations (fig. S1k).[3]

We also grew and characterized thicker $NbSe_2$ films. Unfortunately, we noticed that the quality of few-layer $NbSe_2$ reduces gradually with the number of layers. Figs. S1i and S1j are the ARPES spectra and second-derivative spectra of a 5 ML $NbSe_2$ film. The ARPES spectra of this 5 ML $NbSe_2$ film became significantly more blurred than those of the single layer. However, we still can clearly observe a second band crossing the Fermi level in the second-derivative spectrum (depicted by the blue curve in figs. S1i and S1j). Comparison of this data with theoretical calculations for the bulk $NbSe_2$ band structure[3] allows us to conclude that the additional band in 5 ML $NbSe_2$ is the Nb-derived band of bulk $NbSe_2$, shown in blue in fig. S1k. We did not observe the theoretically predicted Se-derived band

© 2015 Macmillan Publishers Limited. All rights reserved

from bulk $NbSe_2$ shown in green in fig. S1k. However, our ARPES results indicate that single-layer $NbSe_2$ has distinctly different band structure from 5 ML $NbSe_2$.

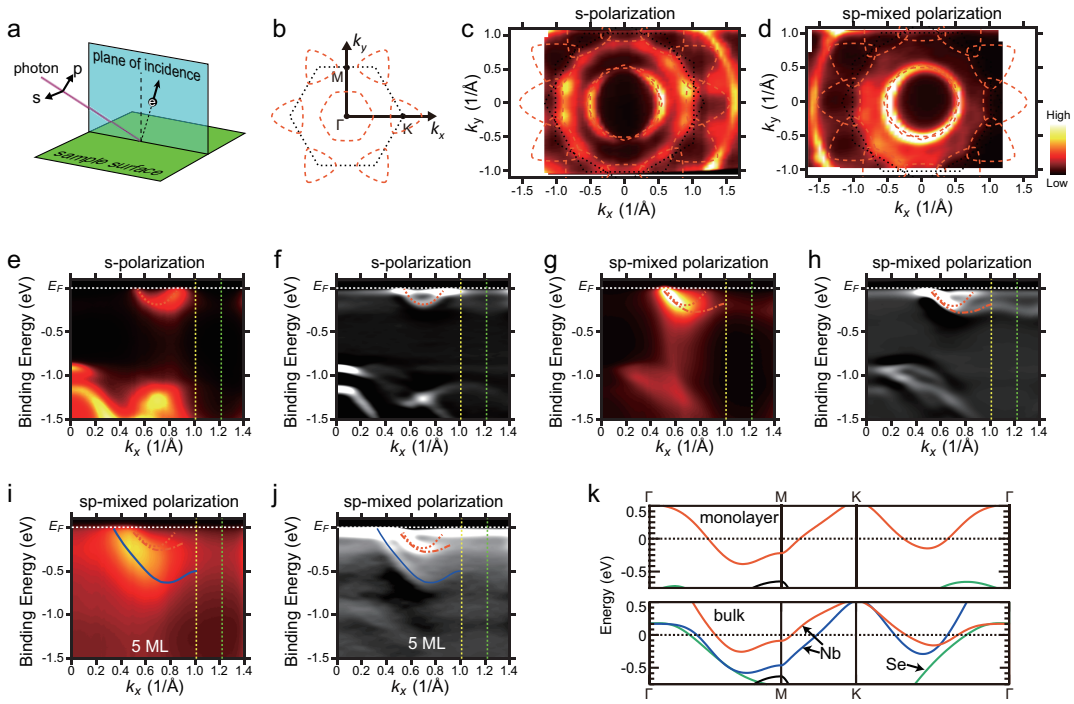

Figure S1: ARPES spectra of $NbSe_2$ films on BLG. a, Schematic drawing of the geometric setting in ARPES measurement. **b,** 2D Brillouin zone (dotted hexagon) and Fermi surface sketch map (orange dotted lines) of single-layer $NbSe_2$. **c,** and **d,** Fermi surface mapping of single-layer $NbSe_2$ film by using *s*-polarization photon and *sp*-mixed polarization photon, respectively; the dotted lines depict the Brillouin zone (black) and Fermi surface (orange) for the two dominantly rotated lattice orientations, respectively. **e,** ARPES spectra and **f**, the second-derivative spectra of monolayer $NbSe_2$ film taken with *s*-polarization photon. **g,** ARPES spectra and **h**, the second-derivative spectra of single-layer $NbSe_2$ film taken with *sp*-mixed polarization photon. The dotted and dot-dashed orange curves indicate bands from the Γ-K and Γ-M directions, respectively. **i,** ARPES spectra and **j**, the second-derivative spectra of 5 ML $NbSe_2$ film taken with *sp*-mixed polarization photon. **k)** Theoretical calculations of the band structures for monolayer and bulk $NbSe_2$ (ref. 2).

© 2015 Macmillan Publishers Limited. All rights reserved

2. Rotational misalignment of single-layer $NbSe_2$ on bilayer graphene

Consistent with our ARPES measurements, domains with multiple rotational alignments with respect to the underlying BLG are seen in the STM images of ML $NbSe_2$. Figs. S2a and S2b show STM images taken on domains with 14° and 22° angles between the $NbSe_2$ atomic lattice and the BLG lattice, respectively. The black arrows lie along the $NbSe_2$ lattice while the red arrows lie along the BLG lattice. Fig. S2c shows an atomically-resolved STM image of the bare BLG substrate, with the atomic lattice directions indicated by red arrows. The LEED pattern for a ML $NbSe_2$ film is shown in Fig. S2d. The red dots correspond to the BLG substrate and show well-defined rotational alignment across the sample. The features corresponding to the $NbSe_2$, however, appear as a smeared-out circle. This circle exhibits increased intensity approximately every 30° as shown by intensity of the LEED pattern in Fig. S2e taken along the black line drawn in the inset. These intensity maxima are aligned at 0° and 30° with respect to the graphene atomic lattice and are sketched as blue (0°) and green (30°) dots in the right side of the LEED pattern of fig. S2d. This is consistent with the ARPES measurements, which indicate two predominant rotational domains separated by 30° that yield two well-defined bands. The observed rotational disorder is a consequence of the weak interaction between the $NbSe_2$ and the underlying BLG substrate and has been observed in other monolayer TMD films grown on BLG.

© 2015 Macmillan Publishers Limited. All rights reserved

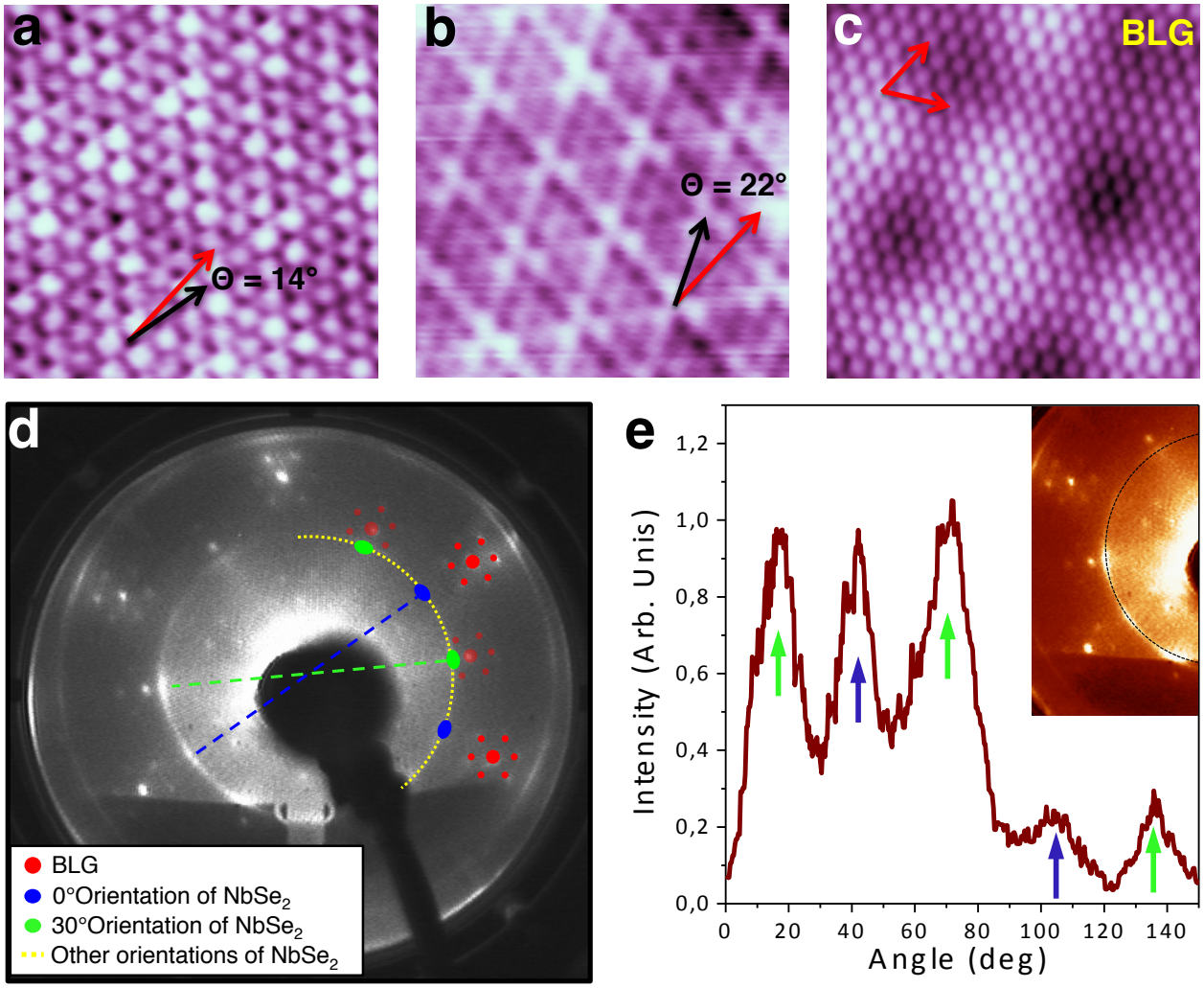

Figure S2: Rotational orientation of monolayer NbSe2 on BLG. Atomically resolved STM images (40 x 40 Å^2) of two domains of the $NbSe_2$ monolayer showing a rotational misalignment of the atomic lattice (black arrow) of **a.** 14° (Vs = - 20 mV, It = 1000 pA) and **b.** 22° (Vs = + 50 mV, It = 50 pA) with respect to the graphene lattice (red arrow). **c.** STM image of the BLG substrate indicating the orientation of the atomic lattice (40 x 40 Å^2, Vs = + 0.1 mV, It = 50 pA). **d.** LEED pattern of monolayer $NbSe_2$ showing the two preferred orientations of $NbSe_2$ (blue and green dots). **e.** Intensity profile of the LEED pattern taken along the arc defined by the black line shown in the inset. The blue and green arrows indicate the maxima of intensity aligned with the atomic lattice of graphene at 0° and 30°, respectively.

© 2015 Macmillan Publishers Limited. All rights reserved

3. Transport measurements

The dc electrical resistance of the sample was measured using a 4-probe contact configuration as shown in Fig. S3.

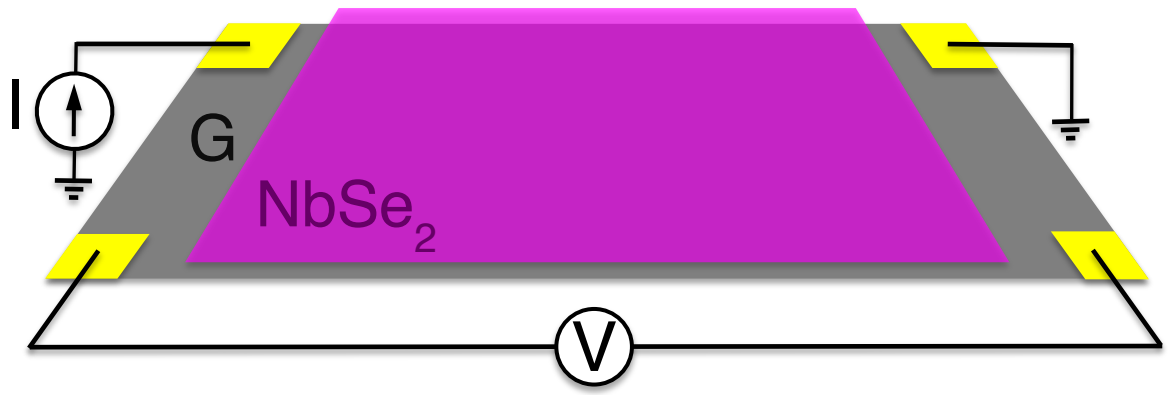

Figure S3: Four-probe configuration for transport measurements. Sketch of the 4-probe contact configuration used in the transport experiments. Graphene (G) layer is shown in grey and NbSe2 in purple. The insulating SiC(0001) substrate is not shown.

References:

1. Damascelli A., Hussain Z., Shen Z.-X. Angle-resolved photoemission studies of the cuprate superconductors. *Rev Mod Phys* 2003, **75,** 473-541.
2. Johannes M. D., Mazin I. I., Howells C. A. Fermi-surface nesting and the origin of the charge-density wave in NbSe2. *Physical Review B* 2006, **73,** 205102.
3. Calandra M., Mazin I. I., Mauri F. Effect of dimensionality on the charge-density wave in few-layer *2H*-$NbSe_2$. *Phys Rev B* 2009, **80,** 241108.

© 2015 Macmillan Publishers Limited. All rights reserved